Proc. Nat. Acad. Sci. USA
Vol. 71, No. 11, pp. 4381–4385, November 1974

Physical and Physiological Evidence for Two Phase Transitions in Cytoplasmic Membranes of Animal Cells

[hydrocarbon spin labels/amino-acid transport/membrane lipids/bilayer structure/ (Na^++K^++Mg^{++})-ATPase/lateral phase separations/membrane asymmetry]

BERNADINE J. WISNIESKI, JOEL G. PARKES, YOSHIE O. HUANG, AND C. FRED FOX

Department of Bacteriology and the Molecular Biology Institute, University of California, Los Angeles, Calif. 90024

Communicated by Harden M. McConnell, August 19, 1974

ABSTRACT **Electron spin resonance analysis of suspensions of animal cell plasma membranes consistently reveals four characteristic temperatures for lateral phase separations in the membrane lipids. Similar analysis of an aqueous dispersion of lipids extracted from these membranes reveals only two characteristic temperatures, indicating that some aspect of lipid organization in membranes is destroyed by the extraction procedure. The characteristic temperatures for surface membranes from two different species of homeothermic animals were nearly identical and were approximately 37°, 31°, 21°, and 15°. A treatment of the physical data revealed that these temperatures could identify independent phase transitions for two hydrocarbon compartments of approximately equal size with lower and upper characteristic temperatures of 21° and 37°, and of 15° and 31°. The analysis of the effects of temperature on a number of physiological parameters indicates that 21° and 37° are likely to define the boundaries for lateral phase separations in the inner monolayer and 15° and 31° the boundaries for lateral phase separations in the outer monolayer.**

Changes in the physical state of lipids affect biological activities in *Escherichia coli* membranes at two characteristic temperatures (1–3). These are analagous to the temperatures that define the boundaries of the phase transition for ideal binary phospholipid systems (4, 5). Below the lower characteristic temperature (t_l) all the membrane lipids are in the solid state. Above the higher characteristic temperature (t_h) all the membrane lipids are in a fluid state. Between t_l and t_h separate solid and fluid phases form in the membrane by a process of lateral phase separation (5, 6). The limits of the temperature range over which lipid hydrocarbon side chains have enhanced lateral compressibility are also defined by t_l and t_h. The alterations in catalytic activities, e.g., transport, that occur at t_l and t_h probably have their origin in the commencement of cooperative interactions at these limits (1).

The physical state of membrane lipids can affect the distribution and mobility of proteins that lie within the hydrocarbon phase. When the temperature is below t_h, but above t_l, these proteins appear to segregate into fluid state lipid domains (7, 8). Below t_l, the rate of lateral diffusion of membrane components is retarded (9–14), but the extent to which it is retarded has not yet been determined with precision. One notable consequence of incubating bacteria below t_l is the cessation of cellular proliferation (9, 15–18).

Abbreviations: ESR, electron spin resonance; 5N10, 2,2-dimethyl,4-butyl,4-pentyl,*N*-oxyloxazolidine; PBS, phosphate-buffered saline; NDV, Newcastle disease virus; MEM, minimal essential medium.

As the first and most logical step in a study of structure–function relationships in animal cell surface membranes, we have used electron spin resonance (ESR) to determine the characteristic temperatures for the lipid phase separation process, and have studied the effects of temperature on a number of biological activities to test for correlations between physical and physiological phenomena.

MATERIALS AND METHODS

Membrane isolation. Cytoplasmic membranes were isolated from mouse LM cells maintained as monolayer cultures in Eagle's minimal essential medium (MEM) plus 0.5% peptone (19). Membranes were isolated as described by Schimmel *et al.* (20) with minor modification (21).

ESR samples and techniques. An aliquot of LM cell plasma membrane (150 μg as membrane protein in 1 mM triethanolamine·HCl, pH 7.4) was prepared for ESR immediately after isolation. Newcastle disease virus, strain HP-16 (NDV_{HP}), was propagated in embryonated chick eggs and purified according to Samson and Fox (22). Polyacrylamide gel electrophoresis of sodium dodecyl sulfate solubilized virus revealed only viral protein bands. Total lipids were extracted from 600 μg (as protein) of NDV by the method of Bligh and Dyer (23). The lipid extract (0.4 ml) was filtered through Na_2SO_4 and glass wool, dried under a stream of nitrogen gas, and suspended in 80 μl of chloroform:methanol (2:1). Aliquots of 10 μl were repeatedly added to a small glass capillary and dried under N_2. When the entire sample had been transferred to the capillary and dried, 12 μl of a solution 1 mM in triethanolamine·HCl, 0.1 mM in $K_3Fe(CN)_6$ and 0.3 mM in spin label were added. The spin label 5N10, a nitroxide-substituted decane (24), was a gift from Dr. A. D. Keith, Pennsylvania State University. ESR spectra were taken as described below for membranes. Membrane or viral suspensions containing 75 μg of protein were combined with 2 μl of 10 mM K_3 Fe $(CN)_6$ and equilibrated at 22° for 30 min. Next, 0.5 μl of the stock solution of 5N10 (2,2-dimethyl, 4-butyl, 4-pentyl, *N*-oxyloxazolidine, 10 mM in ethanol) was added and the sample was incubated for an additional 30 min. The sample was added to a 9 cm long capillary tube which was centrifuged in a swinging bucket rotor at 16,300 × *g* for 1–2 hr at 5°. Supernatant fluid was removed from the capillary until a 1:1 (v/v) ratio of supernatant to pellet volume was attained and the capillary was incubated at 0° for at least 60 min before taking the first ESR spectrum. Spectra were taken in ascending order from approximately 3–43°. Each sample was incubated for at least 10 min at the indicated

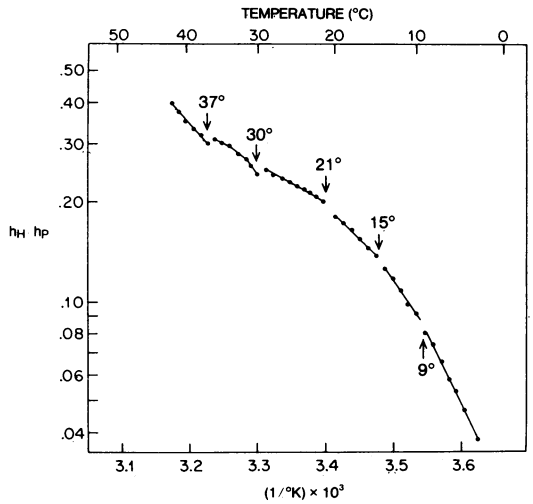

FIG. 1. Characteristic temperatures for the partitioning of the spin label 5N10 between the fluid hydrocarbon phase of LM cell plasma membranes and the surrounding aqueous environment. A decrease in the value of h_H/h_P indicates a loss of spin label from the hydrocarbon phase. The symbols h_H and h_P identify the amplitudes of the hydrocarbon and polar components of the high field line of the first derivative ESR spectrum.

temperature, and each spectrum was a 5 min scan over a 100-G range.

RESULTS

Physical State of Lipids in Membranes. The most thoroughly characterized spin label probe for determining the characteristic temperatures of lipid phase transitions is TEMPO (1, 5). This probe has nearly equal solubility in aqueous and fluid hydrocarbon phases, but little solubility in a frozen hydrocarbon phase. In the present study we have used the spin label 5N10, which is 50-fold more soluble in the hydrocarbon phase than in water. This reduces the requirement for membrane or lipid sample by a like amount. Linden *et al.* reported that t_h was not always revealed when 5N10 was employed (24). This was a consequence of the experimental conditions. When bacterial membrane samples were analyzed by ESR precisely as described in *Materials and Methods* with 5N10 as probe, t_h was always revealed, and the values were precisely (±0.5°) those obtained by use of TEMPO (1) (B. Wisnieski, unpublished).

The characteristic temperatures for the melting of lipids in the surface membranes from a cultured mouse fibroblast line (LM) were determined by ESR (Fig. 1). In contrast to *E. coli* membranes, which commonly exhibit only two characteristic temperatures, five characteristic temperatures were detected. The endoplasmic reticulum fraction prepared from LM cells also exhibited five characteristic temperatures which agreed closely with those detected with cell surface membranes (Table 1) (21). We also assessed the characteristic temperatures of the membrane of Newcastle disease virus, which, like other members of the paramyxovirus group, derives its membrane lipids from the host cell (chicken chorioallantoic) surface membrane (33, 34). ESR studies with NDV revealed four characteristic temperatures which were almost identical to the four highest characteristic temperatures of LM cell surface membranes (Fig. 2, Table 1). This indicates that the surface

TABLE 1. *Physical and physiological characteristic temperatures of animal cell membranes*

5N10 Partitioning	Characteristic temperatures (°C)[a] $t_{l(o)}$	$t_{l(i)}$	$t_{h(o)}$	$t_{h(i)}$
LM plasma membrane	15	21	30	37
Egg-grown NDV_{HP}	14	22	32	38
LM endoplasmic reticulum (21)	16	22	32	38
Physiological parameters	$*t_{l(o)}$	$*t_{l(i)}$	$*t_{h(o)}$	$*t_{h(i)}$
α-Aminoisobutyrate transport (LM cells)	16	20	29	37
$(Na^+ + K^+ + Mg^{++})$-ATPase (LM cell plasma membrane)	15	23	28–31	37
Concanavalin A binding by LM cells (25, 29)	15–19			
Concanavalin A binding by Py3T3 cells (30)	15			
Concanavalin A-mediated hemadsorption by LM cells (25, 29)	13–15			
Concanavalin A-mediated agglutination with Py3T3 cells (31)	15			
Basal adenylate cyclase of rat liver[b]		22	—	36–38
Hormone-stimulated adenylate cyclase of rat liver (32)[b]		22	32	?
Rate of mixing of mouse and human cell surface antigens after cell fusion (14)	15[c]	21	28–30	
Cessation of growth of LM cells[d]		23		

[a] The symbols $t_{l(o)}$, $t_{l(i)}$, $t_{h(o)}$ and $t_{h(i)}$ refer to the lower characteristic temperatures of the outer and inner cell surface membrane monolayers and the upper characteristic temperatures of the outer and inner cell surface membrane monolayers, respectively. Symbols preceded by an asterisk denote physiological characteristic temperatures. The assignment of two sets of characteristic temperatures is based on the calculations given in Table 2, and the assignments of these sets to the inner and outer monolayers of the cell surface membrane are based on the physiological parameters presented in this table. The rationale for these assignments is presented in *Discussion*.

[b] The characteristic temperature for basal adenylate cyclase at approximately 22° was observed by J. Keirns (personal communication). The characteristic temperature at approximately 36°–38° can be detected in Fig. 1 of the data published by Keirns *et al.* (32). The published data do not preclude a characteristic temperature for hormone-stimulated activity at 36°–38°, and the lowest temperature for activity analysis was 20° in the published experiments.

[c] The rate of antigen mixing, a measure of protein mobility on the cell surface, decreased slowly from 42° to 30°. Below 30°, the rate of antigen mixing declined rapidly to a minimum at 21° and then increased from 21° to 15°. A precipitous drop in the rate of mixing occurred below 15°.

[d] Cells for the inoculum were grown at 37° in MEM + peptone (*Materials and Methods*), and tests for growth at various temperatures were also in MEM + peptone (H. G. Rittenhouse and R. E. Williams, unpublished observations).

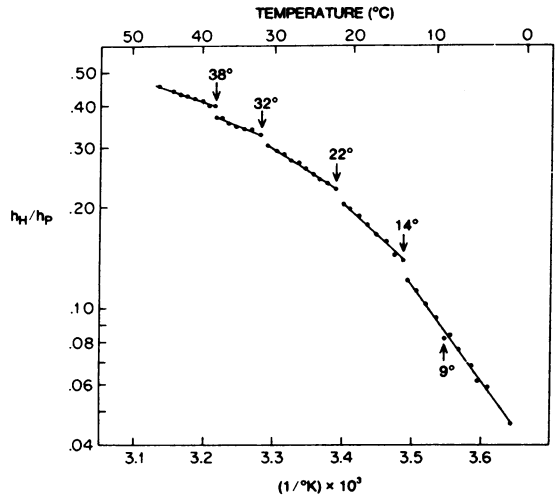

FIG. 2. Characteristic temperatures for the partitioning of the spin label 5N10 between the fluid hydrocarbon phase of membranes of NDV_{HP} virions and the surrounding aqueous environment. A decrease in the value of h_H/h_P indicates a loss of spin label from the hydrocarbon phase. The spectra were taken in ascending order as described in *Materials and Methods*. Scanning in descending order yielded characteristic temperature values identical (±0.5) to those obtained in ascending scans.

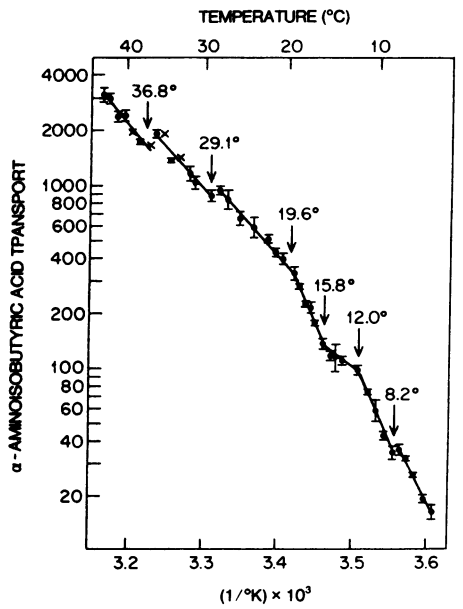

FIG. 3. Arrhenius plot for the rate of α-aminoisobutyric acid transport by LM cells. The range of duplicate values, indicated by the vertical bars, was usually within 5% of the mean (●). Units of activity for aminoisobutyrate uptake are cpm/mg of protein per min of uptake period. Monolayer cultures of LM cells were grown to confluency in MEM + 0.5% peptone in 35-mm wells (25). Growth medium was aspirated from the wells, and the cells were washed with phosphate-buffered saline [PBS (26)]. The trays were incubated at the desired temperature with 1 ml of PBS for 10 min. PBS was removed, and transport assay was initiated by the addition of 0.15 μCi (0.5 ml) of 5 mM [1-^{14}C]-aminoisobutyrate (Amersham/Searle) in PBS. Reactions were terminated by removing isotope solution and adding ice-cold PBS to each well. Each well was washed four times with 5-ml portions of ice-cold PBS. A 1-ml portion of 5% trichloroacetic acid was added to each well, and the samples were incubated for 2 hr at 4°. Radioactivity in aliquots of the acid-soluble fraction was determined by scintillation counting (16). Specific uptake was based on the amount of protein in the acid-insoluble fraction (27). Duplicate assays were performed at each time point, and six time points at each temperature.

membranes of different homeothermic vertebrates have similar physical properties.

Physical State of the Extracted Membrane Lipids. The partitioning of 5N10 between the fluid hydrocarbon and polar compartments of an aqueous dispersion of phospholipids extracted from NDV membranes was studied to determine the effects of membrane organization on the melting behavior of the membrane lipids (*Materials and Methods*). Experiments similar to those described in Figs. 1 and 2 revealed only two characteristic temperatures, a t_h value of 34–35° and a t_l value which ranged from 14° to 17° in a number of studies with independently prepared aqueous phospholipid dispersions.

Characteristic Temperatures for Membrane-Associated Activities. The effects of temperature on the rates of α-aminoisobutyric acid transport and ATPase activity were determined with LM cells and LM cell plasma membrane preparations, respectively (Figs. 3 and 4). Arrhenius plots describing the relationships between the activities of these systems and temperature revealed four characteristic temperatures which correlate with the four characteristic temperatures consistently detected with cell surface membrane preparations (Figs. 1 and 2 and Table 1). Two additional changes or discontinuities in the slopes of these Arrhenius plots occur near the fifth and lowest characteristic temperature detected in LM cell surface membrane preparations by ESR. One or both of these two lowest physiological characteristic temperatures could be generated by the physical event detected in LM cell surface membrane preparations at 9° (Fig. 1).

DISCUSSION

The lipids in the surface membrane of mouse fibroblasts or the membranous envelope of Newcastle disease virus consistently displayed four characteristic temperatures by spin label partitioning (Figs. 1 and 2). The extracted membrane lipids, on the other hand, displayed two entirely new characteristic temperatures, an indication that the lipids of these membranes are organized in a unique and specific fashion. If the four characteristic temperatures of the membranes are all boundaries of lipid phase transitions, the membrane lipids must be sequestered into separate domains of differing composition. These separate domains could coexist within a given monolayer or be disposed in different monolayers. We have considered the latter possibility, since it specifies a condition that can be tested directly by our spin resonance data, the existence of two hydrocarbon compartments of approximately equal size.

Given the values of h_H at temperatures defining the boundaries of two separate phase transitions, the relative sizes (Δh_H^* values) of the two hydrocarbon compartments with phase transitions defined by these boundaries can be compared (Table 2). The major physical assumption implicit in these calculations is that $h_H/°C$ is constant throughout the entire course of a lipid phase transition, and this is approximately true in some instances. The ratios of the values of $h_H/°C$ were calculated from the top and bottom halves of the lipid phase transitions for bacterial membranes and the ex-

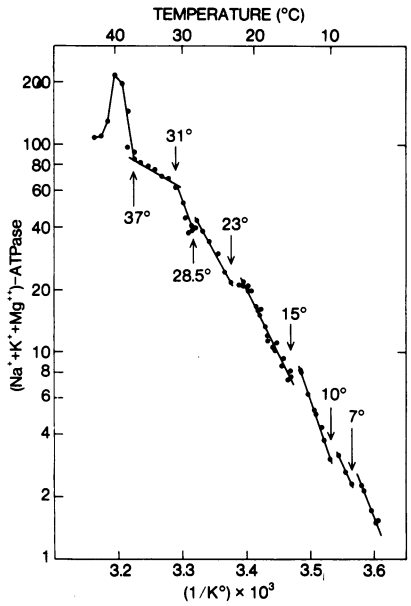

FIG. 4. Arrhenius plot for the rate of $(Na^+ + K^+ + Mg^{++})$-ATPase activity of purified LM cell plasma membranes. Units of activity are μmol of P_i released from ATP per min/mg of membrane protein. Activity was determined in the absence of ouabain in a 0.1-ml system identical in composition to that described by Schimmel *et al.* (20). Reactions were terminated by the sequential addition of 100 μl of Trition X-100 (5% w/v) and 800 μl of a reagent consisting of ammonium molybdate (0.31%), ascorbic acid (1.25%) and H_2SO_4 (0.75 N). The mixture was then incubated at 37° for 15 min and rapidly cooled to room temperature before the absorbance was read at 750 nm. This method of P_i determination is an adaptation of the procedure of Chen *et al.* (28).

tracted lipids from NDV membranes; these ratios (top/bottom) did not exceed a value of 1.25 (B. Wisnieski, unpublished data).

Using the spin resonance data obtained with Newcastle disease virus, we have calculated the values of Δh_H^* for those eight pairs of phase transition boundaries with possible characteristic temperatures of 9°, 14°, 22°, 32°, and 38° (Table 2), for which the temperatures 14°, 22°, and 32° are included in each pair of boundaries. The decision to restrict our treatment to sets of temperatures including these three was based on the reasoning that characteristic temperatures for a change in the temperature coefficient of a lateral diffusion process are almost certain to be phase transition boundaries. Petit and Edidin have experimentally demonstrated that the temperature coefficient for the rate of mixing of mouse and human cell surface antigens after cell fusion is markedly altered at these three temperatures (14). We have included 9° as a possible phase transition boundary since the 9° point was always displaced from the plot of h_H/h_P versus 1/°K for NDV membranes (Fig. 2), and a change in slope was detected at this temperature with LM cell surface membranes (Fig. 1).

Only three pairs of phase boundaries (models 1, 2, and 8) come within a factor of two in satisfying the condition of two hydrocarbon compartments of approximately equal size. Model 1 also satisfies a corollary condition: the sum of h_H/°C values for the nonoverlapping regions of the two phase transitions is equal to the value of h_H/°C in the overlapping region (Table 2). In order to further decide between these three models and to attempt to assign an inner versus outer monolayer

TABLE 2. *Assessment of possible boundaries[a] for lateral phase separations of lipids in membranes of NDV_{HP} virions*

Model	Phase boundaries t_l to t_h = °C*	Interval (°C) for calculation of h_H/°C	h_H[b]/°C	Δh_H*[c]
1	(22 to 38) = 16	(32 to 38)	0.11/6 = 0.018	0.29
	(14 to 32) = 18	(14 to 22)	0.16/8 = 0.020	0.36
2	(14 to 32) = 18	(22 to 32)	0.38/10 = 0.038	0.68
	(9 to 22) = 13	(9 to 14)	0.39/5 = 0.078	1.01

[a] Six other sets of boundaries were considered. These are: model 3, (14° to 38°) and (22° to 32°) which gave Δh_H^* values of 0.46 and 0.19; model 4, (14° to 22°) and (9° to 32°) which gave <0 and >0.87; model 5, (14° to 32°) and (14° to 22°) which gave >0.36 and <0; model 6, (14° to 32°) and (22° to 32°) which gave 0.36 and 0.18; model 7, (14° to 22°) and (22° to 32°) which gave 0.16 and 0.38; model 8, (14° to 22°) and (32° to 38°) which gave 0.16 and 0.11. A detailed description of the procedures used for calculating the Δh_H^* values for models 1–8 will be published elsewhere (21).

[b] The values of h_H at the five possible characteristic temperatures exhibited by spin-labeled NDV_{HP} (see *Materials and Methods*, also Fig. 2) were: 38°, 1.62 cm; 32°, 1.51 cm; 22°, 1.13 cm; 14°, 0.97 cm; and 9°, 0.58 cm.

[c] h_H/°C × °C* = Δh_H*.

localization for each set of boundaries, the physical models have been considered in light of physiological characteristic temperatures (Table 1). Two membrane processes that should be catalyzed by components that span the membrane are Na^+-K^+ transport and aminoisobutyric acid transport. Both aminoisobutyrate transport and plasma membrane-associated ATPase activities are affected at all the characteristic temperatures. The effects of temperature on adenylate cyclase activity allows tentative assignment of a set of boundary temperatures to each monolayer. Keirns *et al.* have published evidence (summarized in Table 1) showing that glucagon and epinephrine stimulated adenylate cyclase activities have a characteristic temperature at 32°, but basal adenylate cyclase activity does not. Since hormone receptors are localized on the outer cell surface, a characteristic temperature of 30°–32° is likely to be a property of the outer monolayer.

The characteristic temperatures for the rate of mixing of cell surface antigens after fusion of mouse and human cells is consistent with models 1 or 8, which best explain the increase in rate of cell surface antigen mixing between 21° and 15° (Table 1). Petit and Edidin favored a model similar to 8, concluding for example that membrane antigens might have less space to traverse the remaining fluid lipid phase as the membrane lipids freeze between 21° and 15°. This increase in rate of antigen mixing is also quite consistent with model 1. If the antigens being scored for mixing penetrate into both monolayers, they would tend to become concentrated in areas of the membrane where opposing monolayers consist entirely of fluid lipid when the membrane consists of a mixture of frozen and fluid lipid phases.† This could give rise to an ex-

† Membrane proteins separate laterally into the remaining fluid lipid phase as the membrane freezes (7, 8). For a general treatment of the physiological effects of lipid phase transitions, see ref. 3.

traordinarily high temperature coefficient for mixing near 21°, since movement of an antigen through a channel of fluid lipid in one monolayer could be retarded by a barrier of frozen lipid in the opposing monolayer. Below 21°, this situation could be relieved by displacement of antigen molecules totally from the inner monolayer into fluid regions of the outer monolayer. This displacement would occur near the lower characteristic temperature for the inner monolayer and, as observed, could give rise to an increased rate of antigen mixing as the temperature is decreased from 21° to 15°. The abrupt decrease in rate of antigen mixing below 15° is consistent with freezing of the outer monolayer at this point. The characteristic temperature for cellular proliferation at 23° is consistent with either of models 1 or 2. Bacterial growth has clearly been shown to cease at the lower characteristic temperature of the lipid phase transition. Since a membrane of totally frozen lipids is apparently incompatible with the ability of bacteria to proliferate, it is likely that animal cells would cease to grow and divide when either one or both monolayers of the bilayer became frozen.

On the basis of the best agreement with the aggregate of physical and physiological data, we favor model 1, in which the characteristic temperatures are 22° and 38° for the inner monolayer and 14° and 32° for the outer monolayer of the membranous envelope of NDV. Similar characteristic temperatures (±2°) can be assigned to the inner and outer monolayers of the LM cell surface membrane, and this very same model best fits the ESR data for LM cell endoplasmic reticulum (21). This physical asymmetry has a compositional precedent in human erythrocyte membranes, where the bulk of the choline containing phosphatides is apparently localized on the outer monolayer, and phosphatidylserine and phosphatidylethanolamine are on the inner monolayer (35, 36). Our data indicate that asymmetry based on lipid sidedness extends not only to the surface membranes of cells other than erythrocytes, but to the internal membranes of these cells as well. Though the physiological significance of this asymmetry is not obvious at this point, the characteristic temperature at or slightly below body temperature may be of interest. Homeothermic animals are known to have body temperature fluctuations in the circadian cycle (37). The increase in rate with decreasing temperature that occurs at 37° for aminoisobutyrate transport (Fig. 3), and probably for other membrane-associated processes as well, might facilitate a rebound or recovery from the low point in the circadian cycle.

This work was supported by Research Grants GM-18233 and AI-10733 from the United States Public Health Service. C.F.F. is the recipient of United States Public Health Service Career Development Award GM-42359, B.J.W. is a Celeste Durand Rogers Postdoctoral Fellow and J.G.P. a Postdoctoral Fellow of the Damon Runyon Fund.

1. Linden, C. D., Wright, K. L., McConnell, H. M. & Fox, C. F. (1973) *Proc. Nat. Acad. Sci. USA* **70**, 2271–2275.
2. Machtiger, N. A. & Fox, C. F. (1973) *Annu. Rev. Biochem.* **42**, 575–600.
3. Fox, C. F. (1974) in *Cell Walls and Membranes, MTP Reviews of Science: Biochemistry*, ed. Fox, C. F., (Butterworths, London), in press.
4. Phillips, M. C., Ladbrooke, B. D. & Chapman, D. (1970) *Biochim. Biophys. Acta* **196**, 35–44.
5. Shimshick, E. J. & McConnell, H. M. (1973) *Biochemistry* **12**, 2351–2360.
6. Shimshick, E. J., Kleemann, W., Hubbell, W. L. & McConnell, H. M. (1973) *J. Supramolecular Struct.* **1**, 285–294.
7. Kleemann, W. & McConnell, H. M. (1974) *Biochim. Biophys. Acta* **345**, 220–230.
8. Kleemann, W., Grant, C. W. M. & McConnell, H. M. (1974) *J. Supramolecular Struct.*, in press.
9. Tsukagoshi, N. & Fox, C. F. (1973) *Biochemistry* **12**, 2822–2829.
10. Chen, Y. S. & Hubbell, W. L. (1973) *Exp. Eye Res.* **17**, 517–532.
11. Jan, L. & Revel, J. P. (1974) *J. Cell Biol.* **62**, 257–273.
12. Nicolson, G. L. (1973) *Nature New Biol.* **243**, 218–220.
13. Rosenblith, J. S., Ukena, T. E., Yin, H. H., Berlin, R. D. & Karnovsky, M. J. (1973) *Proc. Nat. Acad. Sci. USA* **70**, 1625–1629.
14. Petit, V. A. & Edidin, M. (1974) *Science* **184**, 1183–1185.
15. Overath, P., Schairer, H. U. & Stoffel, W. (1970) *Proc. Nat. Acad. Sci. USA* **67**, 606–612.
16. Tsukagoshi, N. & Fox, C. F. (1973) *Biochemistry* **12**, 2816–2822.
17. McElhaney, R. N. (1974) *J. Mol. Biol.* **84**, 145–157.
18. McElhaney, R. N. (1974) *J. Supramolecular Struct.*, in press.
19. Wisnieski, B. J., Williams, R. E. & Fox, C. F. (1973) *Proc. Nat. Acad. Sci. USA* **70**, 3669–3673.
20. Schimmel, S. D., Kent, C., Bischoff, R. & Vagelos P. R. (1973) *Proc. Nat. Acad. Sci. USA* **70**, 3195–3199.
21. Wisnieski, B. J., Huang, Y. O. & Fox, C. F. (1974) *J. Supramolecular Struct.* **2**, in press.
22. Samson, A. C. R. & Fox, C. F. (1973) *J. Virol.* **12**, 579–587.
23. Bligh, E. G. & Dyer, W. J. (1959) *Can. J. Biochem. Physiol.* **37**, 911–917.
24. Linden, C. D., Keith, A. D. & Fox, C. F. (1973) *J. Supramolecular Struct.* **1**, 523–534.
25. Rittenhouse, H. G. & Fox, C. F. (1974) *Biochem. Biophys. Res. Commun.* **57**, 323–330.
26. Weber, M. J. (1973) *J. Biol. Chem.* **248**, 2978–2983.
27. Lowry, O. H., Rosebrough, N. J., Farr, A. L. & Randall, R. J. (1951) *J. Biol. Chem.* **193**, 265–275.
28. Chen, P. S., Jr., Toribara, T. Y. & Warner, H. (1956) *Anal. Chem.* **28**, 1756–1758.
29. Rittenhouse, H. G., Williams, R. E., Wisnieski, B. & Fox, C. F. (1974) *Biochem. Biophys. Res. Commun.* **58**, 222–228.
30. Noonan, K. D. & Burger, M. M. (1973) *J. Biol. Chem.* **248**, 4286–4292.
31. Noonan, K. D. & Burger, M. M. (1973) *J. Cell Biol.* **59**, 134–142.
32. Keirns, J. J., Kreiner, P. W. & Bitensky, M. W. (1973) *J. Supramolecular Struct.* **1**, 368–379.
33. Choppin, P. W., Klenk, H.-D., Compans, R. W. & Caliguiri, L. A. (1971) in *Perspectives in Virology*, ed. Pollard, M., (Academic Press, New York), Vol. VII, pp. 127–157.
34. Blough, H. A. & Lawson, D. E. M. (1968) *Virology* **36**, 286–292.
35. Bretscher, M. S. (1972) *Nature New Biol.* **236**, 11–12.
36. Verkleij, A. J., Zwaal, R. F. A., Roelofsen, B., Comfurius, P., Kastelijn, D. & van Deenen, L. L. M. (1973) *Biochim. Biophys. Acta* **323**, 178–193.
37. Brobeck, J. R. (1960) in *Medical Physiology and Biophysics*, eds. Ruch, T. C. & Fulton, J. F., (W. B. Saunders, Philadelphia), 18th ed., pp. 992–993.